A REVISED TECTONIC MODEL OF MINAHASA DISTRICT BASED ON LiDAR, IMAGE LOG AND FRACTURE STABILITY ANALYSIS IN TOMPASO

Muhammad Ikhwan[1], Mochamad H. Thamrin[1] & Imam B. Raharjo[1]

[1] PT. Pertamina Geothermal Energy, Skyline Building, Jl. M. H. Thamrin no.9, Jakarta, Indonesia

ikhwan.aziz@pertamina.com

Keywords: *Tompaso, Sulawesi, Tondano, tectonic, permeability, geology, geothermal system, structure, geomechanics*

ABSTRACT

This paper investigates the tectonic setting of the Minahasa district by using the updated surface and subsurface data of the Tompaso geothermal field, North Sulawesi, Indonesia. The update includes a detailed analysis of the high-resolution surface topographic map, a borehole image structural interpretation, feedzone identification from the well-test, and stress analysis from the geomechanics study. These methods lead us to a new tectonic concept of the Minahasa district, which consistent with the geothermal conceptual model in the Tompaso area. In line with this, we also evolve the previous well-known literature of Minahasa district tectonic as we used more detailed surface and subsurface data.

This paper assesses subsurface geology uncertainty in the Minahasa district, which is mainly hindered by surface interpretation. We argue the local ENE-striking fault existence that suggested by previous literature. We define the local Minahasa district on surface and subsurface, dominantly controlled by NE-striking fractures due to North Sulawesi subduction and East Sangihe subduction. The geomechanics study describes the regional and local stress direction to construct our tectonic concept and corroborates the local Tompaso area's structural framework. This interpretation also supports the mechanism of Tondano Caldera forming explanation as a classic ellipsoidal natural collapse caldera that follows the maximum horizontal stress trend, rather than occurring as a result of the step-over mechanism. Our permeability investigation through detailed integrated analysis of the borehole image with the injection spinner data suggests the NE-trend fluid flow direction, either from reservoir scale or well scale without showing a robust existence of ENE-striking fractures.

1. INTRODUCTION

Minahasa district is situated in the northern arm of Sulawesi island, Indonesia. Its surrounded by Tondano Caldera in the east and the Soputan volcanic complex in the west. Minahasa district comprised a geothermal area called Tompaso field, which is owned and operated by PT. Pertamina Geothermal Energy (PGE). PGE drilled several wells to confirm the geothermal resource in the Tompaso field and proved a viable high-temperature geothermal resource with benign fluid that economically prospect. PGE also runs the borehole image logging in two wells within the drilling activity that gives insight into subsurface geology in the Tompaso area.

The reference and publication of regional tectonic settings in the local Tompaso area are limited, but a detailed satellite image analysis was published by (Lécuyer et al., 1997). It proposed a structural model in the eastern end of the North Sulawesi that controlled the occurrence of 20x10 km² Tondano caldera. Lécuyer et al. (1997) interpreted the Tondano caldera formed by active ENE-WSW left-lateral strike-slip fault as the transfer fault between the W-E North Sulawesi subduction in the north with the N-S Sangihe subduction in the east. These strike-slip faults formed the stepover, resulting in Tertiary NE-SW trending faults reaction to the pull-apart basin mechanism that precursor the Tondano volcanic activity.

We argue this hypothesis as we find new evidence from the updated imagery data such as LiDAR and IFSAR which shown abundant NE striking lineament and agrees with the interpreted dominant fractures trend inside the local Tondano caldera. We also combine the surface geological data with the subsurface data from the drilling activity and geophysics analysis to analyze the geology beneath the ground focusing on the existing structural trend. We propose a tectonic concept update of the North Sulawesi eastern arms area, contributing to the local geothermal system, especially in the Tompaso field.

2. REGIONAL GEOLOGY SETTING

Katili (1991) described the Sulawesi formed due to the northward Australian plate movement and the New Guinea movements anticlockwise movement in Neogene. The northern arm is composed of late Paleogene to Neogene subduction-related volcanic arc rocks resulting from the west-dipping subduction of the Molucca Sea Plate and south-dipping subduction Sulawesi Sea Plate (Satyana et al., 2011). The K-shaped island of Sulawesi comprises northern arms of tertiary sediments and volcanic-arc rocks, eastern arms of Cretaceous and Neogene accretionary-wedge materials (Hamilton, 1979) southern and western arms with Cretaceous accretionary-wedge rocks. Subduction complexes dominate the east and southeast arms (Figure 1.A).

The eastern end of North Sulawesi is a complex subduction area. Tectonic setting and volcanism in this area are controlled by two subductions with a different orientation, the W-E trending North Sulawesi subduction in the north and the N-S trending Sangihe subduction in the east. The latter is a part of the double subduction system and the Halmahera subduction in the Mollucas Sea suture (Hall & Wilson, 2000). The North Sulawesi subduction controls the North Sulawesi arms shape, while the Sangihe subduction triggers the volcanism arc along the eastern end of North Sulawesi. The North Sulawesi area is divided into three compartments: 1) the NE-SW trending compartments (Minahasa compartments), 2) the central E-W trending segment (Gorontalo compartments) and, 3) the N-S trending compartment or Neck (Siahaan et al., 2005). The Minahasa compartment is part of Sangihe Ridge that created an inner volcanic arc.

ISSN 2703-4275

The Minahasa district is dominated by Quaternary and Recent volcanic products lying over the Tertiary volcanic product. The most prominent volcanic structure feature is the Tondano caldera exposed in the eastern part of the Minahasa district. The Tondano erupted during Pliocene – Pleistocene yields 20x10 km² caldera, spreads volcanic product extensively. The Tondano caldera produced two eruption episodes with remarkable volcanic products (Lecuyer et al., 1997). The Domato tuff (TD) was the first eruption product that deposited extensively beyond the caldera. This thick ignimbrite deposit interpreted erupted in Pliocene as it lies on the upper Miocene volcanic deposit. The second eruption product, the Terras tuff (TT), is characterized by the dacitic ignimbrite in the north and north-west valley and inside the caldera. Several volcanic episodes occur due to caldera collapsing block, either inside caldera or through the caldera rim, such as Lahendong volcanic complex erupted in the centre, Rindengan – Sempu volcanic complex on the south, and Mahawu volcanic complex in the north of caldera (Siahaan et al., 2005). These NE-trending volcanoes series extend to the Sangihe arc and the southern Philippines as the post-Tondano volcanism.

Geologic structures in the Minahasa area are mainly controlled by two major strike-slip faults that cut the North Arm of Sulawesi in two places, between Amurang - Malompar in the south Manado - Kema in the north (Effendi & Bawono, 1997). Based on the shape of the western coastline of Minahasa, especially in Manado area, we interpret that the faults moved laterally in the same directions, as the left lateral strike-slip fault. Yet, further analysis is needed to confirm this sense of movement hypothesis.

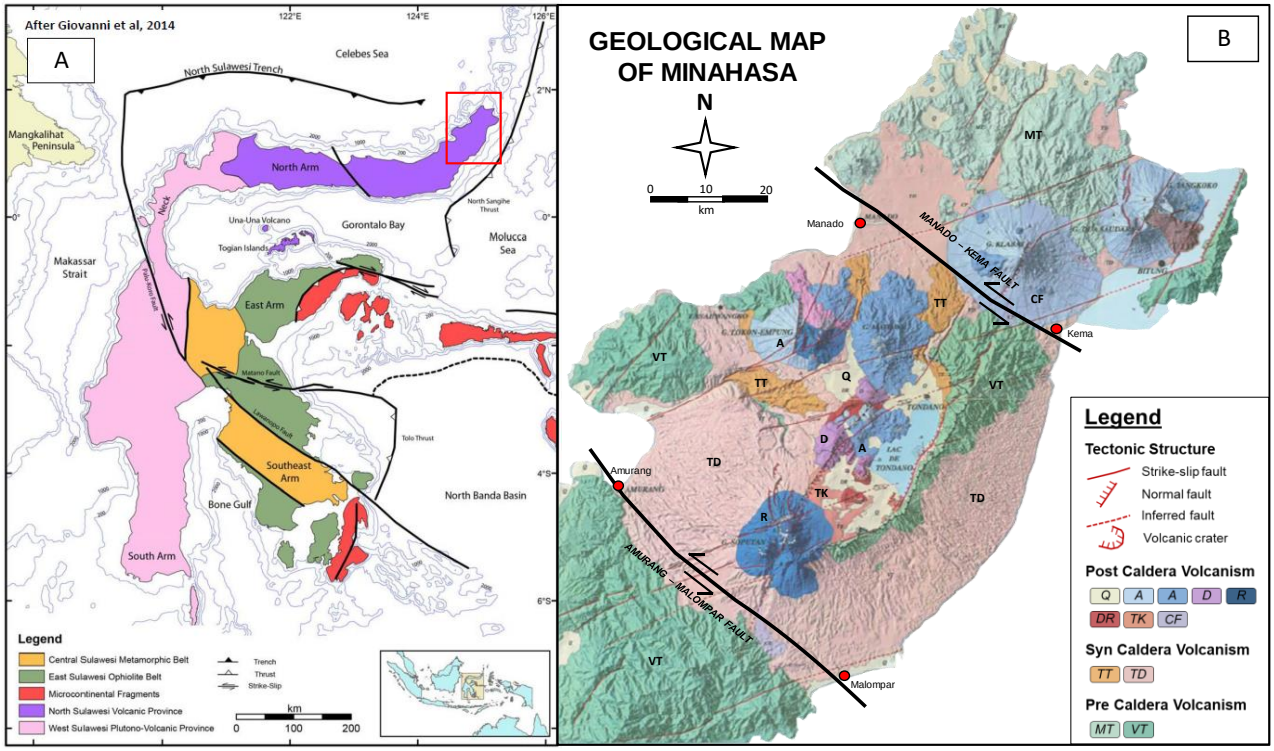

Figure 1: A) The major tectonic settings with four arms distribution of Sulawesi (Szentpéteri et al., 2015, after Pezzati (2014)). The red box is the Minahasa district. The index shows the Indonesia map. B) Geological map of the Minahasa district by Lecuyer et al. (1998) shows the distribution of pre, syn, and post-Tondano caldera products and domination of ENE-WSW structures control and form the caldera collapse oriented to NE-SW. This map combined with the two major strike-slip faults bound the Minahasa district in the northeast and southwest (Effendi and Bawono, 1997).

3. TECTONIC IDENTIFICATION OF MINAHASA DISTRICT

Recently, several literatures have discussed the tectonic and volcano-stratigraphy of the Minahasa district. Utami et al. (2020) and Sidqi and Utami. (2018) explain the geology and the geothermal system in the Minahasa district. Sardiyanto et al. (2015) focusing on the permeability control analysis in the Tompaso field based on the surface and subsurface image log data. The reliable Minahasa tectonic framework that has been used as the reference mostly in these publications is the Lecuyer et al. (1997). It suggests the active ENE-WSW left-lateral strike-slip faults that cross the Minahasa district and influences the Tondano caldera occurrence due to the stepover zone from two parallel strike-slip faults with the same movement (Figure 1.B). Another remarkable active ENE-WSE strike-slip fault interpreted cut the young Soputan volcanic complex that continues to the west while the eastern extent is obscure (the most southern blue volcano in Figure 1.B). These strike-slip faults are assumed as the transfer faults between the Celebes Sea subduction in the north with the Sangihe subduction in the east. The ENE-WSE strike-slip faults accommodate the Tertiary NE-SW fault reactivation that was exposed in the Minahasa district.

Some of the NE-SW fault scraps and lineaments are expressed in the Minahasa district, constructed from the satellite imagery. Regionally, a distinguished NE-SW fault crosses the Minahasa district in the northern part, faulting Mount Tondano as the Lengkoan

ISSN 2703-4275

fault (Figure 2.B). The extension of this fault toward the Rindengan crater may be covered by the younger Quaternary volcanic product of Rindengan since such fault formed during Tertiary. However, it is unclear whether this fault also acts as the Tondano caldera western boundaries or occurred as the post-Tondano caldera structural framework.

As Lecuyer et al. (1997) focus on the satellite imagery analysis, we study the tectonic setting in the Minahasa district from surface and subsurface data in this paper. The surface analysis was derived from the LiDAR imagery analysis to see the detailed terrain model in the local Tompaso area. The subsurface analysis was deducted from the image log data derived from drilling activity. The geophysics study also supports our tectonic interpretation in this area. These data combinations enable us to confirm the existing structural framework in Tompaso.

3.1 LiDAR Imagery Analysis

Overall, the occurrence of the ENE-WSW lineament in the Minahasa district might be more visible as the southern wall of the Tondano caldera (Figure 2.A). For more local investigation, we use LiDAR data available in this study extend 10x20 km², which covers the Tompaso geothermal field, including the G. Soputan volcanic complex in the west and the G. Umeh volcano in the east (Figure 2.B). From LiDAR analysis, the existence of ENE-WSW strike-slip fault in this area is less exposed instead of the short lineaments at some spots which faking to one single ENE-WSE lineament. For instance, an ENE-striking lineament lying on Sempu volcanic complex, later called as Soputan Fault, interpreted as a major strike-slip fault by Lecuyer (1998), might find as a non-tectonic feature. This lineament was actually formed by the combination of the Rindengan Caldera wall and sector collapse on the west with a parallel eruptive vent wall feature on the east, composed by G. Wowok and Luwuk. Moreover, there is almost no ENE-striking displacement in the area between instead of the NE-striking lineament such Panasen Fault. Therefore, we believe these volcanoes caldera and crater wall has faked the tectonic lineament which misleads the interpretation of the active left-lateral strike-slip Soputan Fault in the previous literature.

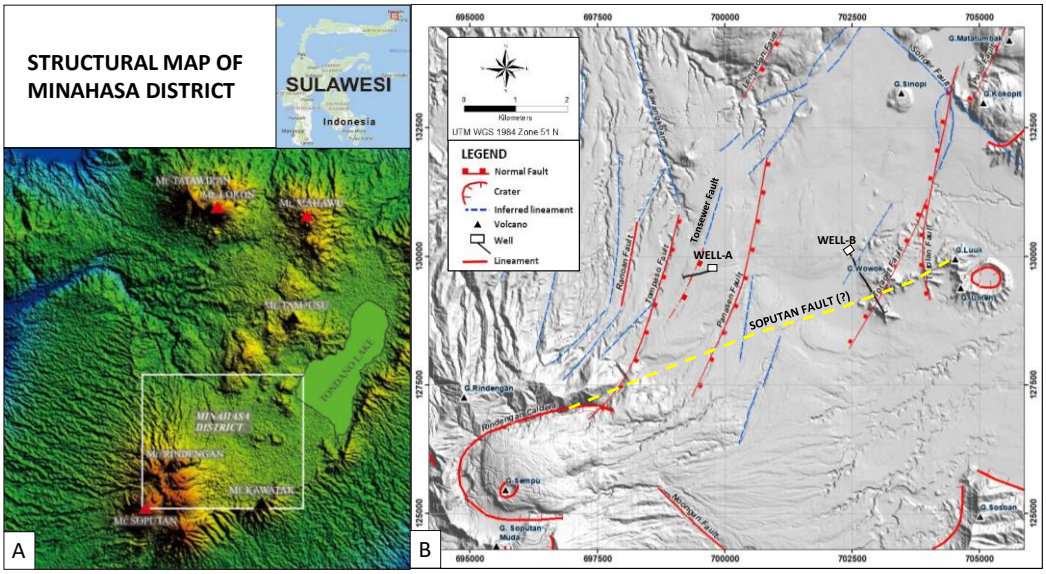

Figure 2: A) Location of Tompaso field at the northern arm of Sulawesi (Sidqi and Utami, 2018). The white box shows the location in B. B) The surface structural analysis of the local Tompaso area by using LiDAR imagery.

On the other hand, the NE-striking lineaments are more robust and visible on LiDAR imagery data. The Tompaso fault remarks the NE-SW fault trend and bound the Rindengan crater rim with G. Sempu lava. A series of parallel lineaments in the west of Tondano Caldera was also exposed, such as Ranoan, Tonsewer, and Panasen lineaments. The LiDAR imagery also highlights a remarkable NW-SE Kawangkoan lineament in the north of the Tompaso fault. It is represented as the distinguish fault scarp or river that also bound the Rindengan volcanic product in the north.

3.2 Image Log and PTS Spinner Analysis

Drilling activity in the Tompaso area provides some image log data that contains information about the subsurface structural trend penetrated by the well. The two image log data are conducted in Well-A and Well-B (Figure 2.B). The image log gives the image of subsurface geology, especially in the production intervals. Raw conductive and resistive fractures orientation analysis of these two image log data shows the domination of the NE-SW trend, either from the Well-A and Well-B (Figure 3). Fractures in the Well-A are mostly clustered in the lower interval that is dominated by the NE-SW trend, while the well is relatively oriented to N250°E. These subsurface fracture orientations may confirm those fault trends existence as the borehole targeted the NE-striking Tompaso lineaments group. We infer the dip azimuth of this fracture group based on the image log data. Another minor fracture trend was recorded in shallower depth which relatively oriented W-E but only in a short interval. The Well-B deviated E45°S, which is relatively perpendicular to inferred Soputan Fault from the previous literature, as the well target, that should increase the probability for this well to intersects such faults zone and we expected such fracture zone will much dense. However, the image log proves that the fractures with such orientation are likely appear minor, although they are exists in the fracture zone 4 but less dominant for the whole log section.

ISSN 2703-4275

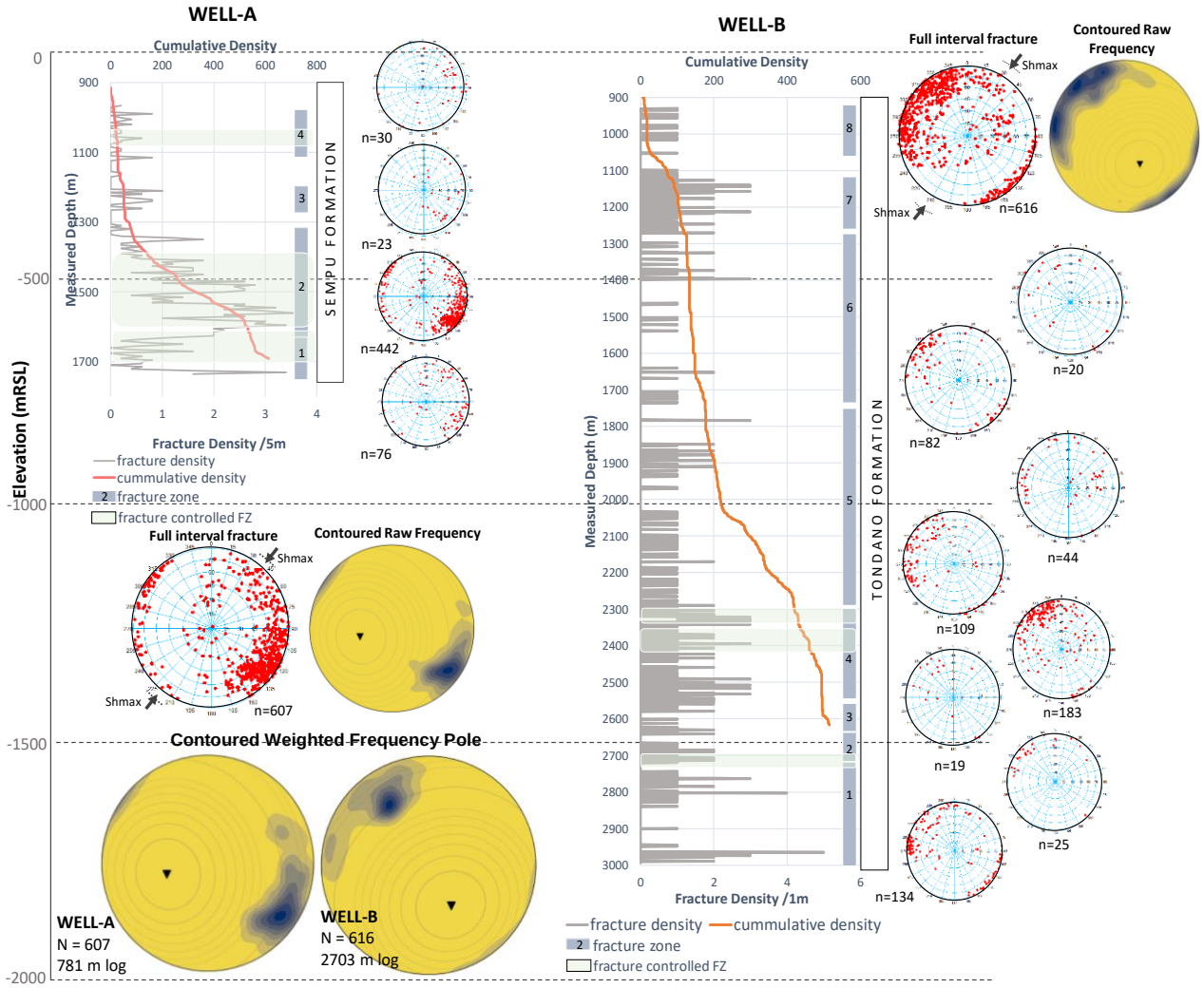

Figure 3: Diagrams of fracture density, orientation, and feedzone (FZ) intervals for wells Well-A and Well-B. Fracture density for each well is plotted as both the moving average density over 5 m and 1 m intervals and cumulative fracture density. Larger stereonets show total well fracture orientations, and smaller stereonets show fracture orientations within each fracture zone in each well. Shaded greenish intervals on the fracture density plots indicate the fault-controlled feedzones identified from the injection spinner test. (Bottom left) The contoured weighted frequency pole.

The NE-SW fractures trend also influences the well-scale permeability in both Well-A and Well-B. The combination of image log and spinner data analysis leads to significant flow in the dense NE-SW fractures intervals. Mostly fracture-controlled feedzone (FZ) dominant in both wells lower depth interval supports the steam production with sufficient output (Table. 1). In Figure 3, the most prominent FZ interval in Well-A associated with fracture zone 2 contains most fractures in the well, dominated by the NE-SW fracture dipping to SE. In Well-B, FZ correlated with fracture zone 2, 4, and the lower part of zone 5. In both wells, the FZ magnitudes are more correlates with the fracture density, as shown in the fracture zone 2 in the Well-A and fracture zone 4 in the Well-B. These zones confirm the existence of NE-SW fractures, included their largerst fracture in the FZ, which are quite different from the ENE-WSW inferred Soputan fault that has been interpreted on the surface from the previous studies.

Table 1. The distribution of fault-controlled feedzones in Well-A and Well-B

Well	Fracture-controlled FZ	Depth (mMD)	Fractures trend	Associated surface fault	Formation
Well-A	Feedzone 1	1020 - 1070	W-E	Tonsewer fault	Sempu
	Feedzone 2	1400 - 1600	NE-SW		
	Feedzone 3	1645 - 1700	NE-SW		
Well-B	Feedzone 1	2301 - 2321	NE-SW	Totolan fault	Tondano
	Feedzone 2	2330 - 2348	NE-SW		
	Feedzone 3	2704 - 2725	NE-SW		

Terzaghi's (1965) concept explains the probability of the fault or fractures that the wells intersected are highly influenced by the angle between the well and the fracture orientation. The concept describes how the fractures that are perpendicular to the well are most likely intersected by the well than those relatively parallel with the well. This called geometric sample bias generates the 'blind zone' of the fracture datasets representing the fractures that parallel with the well and rarely intersected. Terzaghi (1965) proposed a methodology that quantifies the geometric sample bias using the acute angle (alpha) between the fracture plane and the line. Wallis et al. (2020) worked out how to visualize the blind zone (where sin(alpha) +/- 0.3) and contours of sample bias (isogenic contours) on a stereonet by using machine learning code that enables us to visually evaluate the degree that geometric sample bias in affects a fracture dataset in form of contoured weighted frequency pole. Through this method, we confirm that the dominant NE-striking faults orientation in both wells are not a geometric sample bias. From weighted using Terzhagi's concept show the NE-striking fractures acquired in Well-A and Well-B are high-angle, dipping both NW and SE, and aren't likely the geometry sample bias instead lead to structural grain evidence. These drilling activities confirm the existence of the NE-SW trending fault, which is mostly covered by the younger volcanic products, both derived from the Soputan volcanic complex or Umeh volcano.

3.3 Geomechanics Analysis

3.3.1 Drilling-induced fracture rotation

Zoback et al. (1985) found that most permeable faults are critically stressed and active. A method to identify active faults penetrated by drilling activity is proposed by Zoback (2010), who determines the in-situ stress along the borehole by analyzing the presence of drilling-induced fractures (tensile fracture). The stress imbalance causes tensile fractures during drilling due to removing excess pressure at particular depths inside the borehole (related to the drilling fluid such as mud) (Ezer, P., 2008). Tensile fractures usually appear as a pair of narrow, sharply defined features on the electrical image log. Tensile fracture orientation in the image log is strongly dependent on well orientation and inclination.

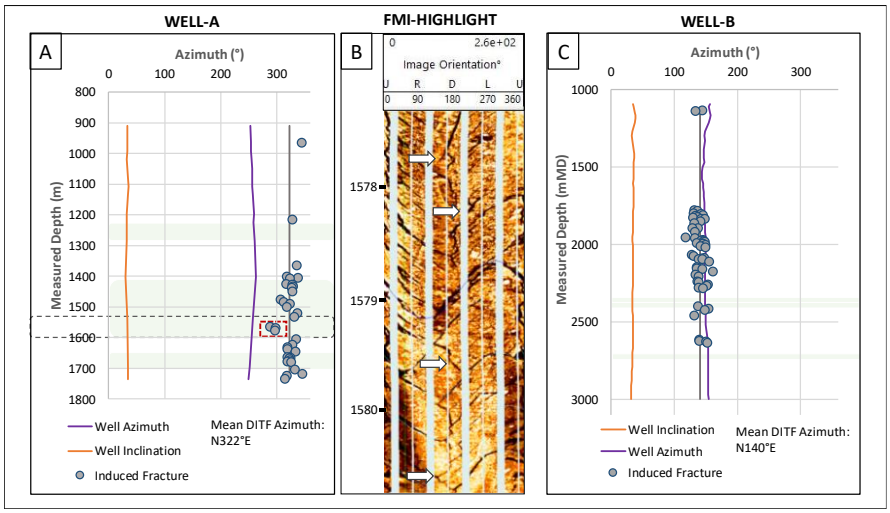

Figure 4: Drilling induced fractures combined with identified feedzones. A) An abrupt rotation detected align with the middle feedzone in Well-A. The black dots show the interval of major induced fracture rotation in Well-A. The red dots show the highlighted interval in B. B) The dynamic image log (FMI) at abrupt induced fracture dip rotation interval in Well-A. The white arrow pointing the steep changes in induce fracture dip due to the active and intensive NE-SW fractures. C) The drilling-induced fractures plot in Well-B relatively have no significant abrupt orientation rotation.

The orientation rotation of these tensile fractures and breakouts can be interpreted geomechanically as the impact of an active fault or fracture zone in the borehole (Zoback et al., 1995). A plot of drilling-induced tensile fractures (DITF) together with the well orientation (inclination and azimuth) is shown in Figure 4. There is a possible rotation in the induced fractures trend in the middle feedzones of Well-A while the well azimuth and inclination remain steady. As this fracture zone is associated with dominant NE-SW fractures, we interpret that the NE-SW fractures in the Tompaso field are the active tectonic movement and contribute to the steep change of drilling-induced fracture orientation in such interval. In contrast, we weren't noticed drilling-induced fracture rotation changes in Well-B, which lead to an assumption that this area might be less tectonically active than Well-A.

3.3.2 Fracture Stability

The stress regime knowledge is critical to synthesize the tectonic setting in an area. In this study, we investigate the stress regime of the Tompaso area by model the fracture stability from the image log data and confirm the model by correlating it to the actual feedzone data. The fracture stability analysis examines the critically stressed fracture, which is interpreted as the permeable fracture or possibly open, by measure its slip tendency ratio (Barton et al., 1995). Once a stress regime is identified, normal and shear stresses on fractures orientation available in image log data can be determined, and their slip tendency could be calculated (Townend & Zoback, 2000).

Fractures with high slip tendency are at an orientation (strike and dip) where they are more likely to experience shear failure given the magnitude and orientation of the effective stress tensor, where the effective stress tensor is the maximum σ1, intermediate σ2, and minimum σ3 tectonic stresses minus the oppositional force of pore fluid pressure. The open and permeable fracture might be associated with the conductive fracture stated in the image log interpretation. Yet, it's important to note that the conductive fracture with a dark appearance on the image log could be interpreted into two things: open fracture or mineral-filled fracture such as clay. We use these conductive fractures data, such as strike and dip, rotating them into the geographical coordinate by using the method from Zoback (2010), to clusters which of those fractures that are critically stressed. Barton et al. (1995) suggest normally the possible stressed open fracture would have the shear to the normal ratio between $\mu = 0.6$ and $\mu = 1.0$. The Tompaso field is modelled as the normal faulting regime area where σ1 = vertical (Andersonian), which fit the actual wells condition. The orientation of maximum horizontal stress (Shmax/ σ2) is derived from focal mechanism analysis (Wardani et al., 2020) and surface structure measurement

(PGE, 2009). This analysis concludes the maximum horizontal stress is mainly oriented to N30°E, which is parallel with the dominant image log's conductive fracture orientation. Drilling-induced fracture orientation in image logs also suggests the relatively NE-SW maximum horizontal stress orientation in both well. However, it is difficult to define maximum horizontal stress from the drilling-induced fracture as the well's inclination is more than 15°.

The fracture and fault data in three dimensional Mohr representations (shear vs effective normal stress normalized by the vertical stress) are shown in Figure 5. As indicated by the Coulomb failure lines $\mu = 0.6$ and $\mu = 1.0$ in the left column, most of the conductive fractures (;70%–80%) in Well-A and ~50% of conductive fractures in Well-B appear to be critically stressed on the normal fault regime model with the maximum horizontal stress oriented to N30°E, which potentially active faults in frictional equilibrium with the in-situ stress field. The middle column is the model from rotated maximum horizontal stress to N75°E, which concludes less of the conductive fractures on both well are critically stressed compares with the N30°E stress orientation. To confirm the stress regime in the local Tompaso area, we also model the strike-slip stress regime (right column) as suggested from previous literature which interprets the ENE-WSW strike-slip fault as the active fault. We use the fault component from focal mechanism analysis to applied as the parameter on the rotated fracture component into the stress state on the strike-slip regime. From this model, the conductive fractures on both wells mostly are non-critically stressed that should not be able to flow the hydrothermal fluid which disagrees the actual condition from the spinner data that indicates both wells are good in permeability.

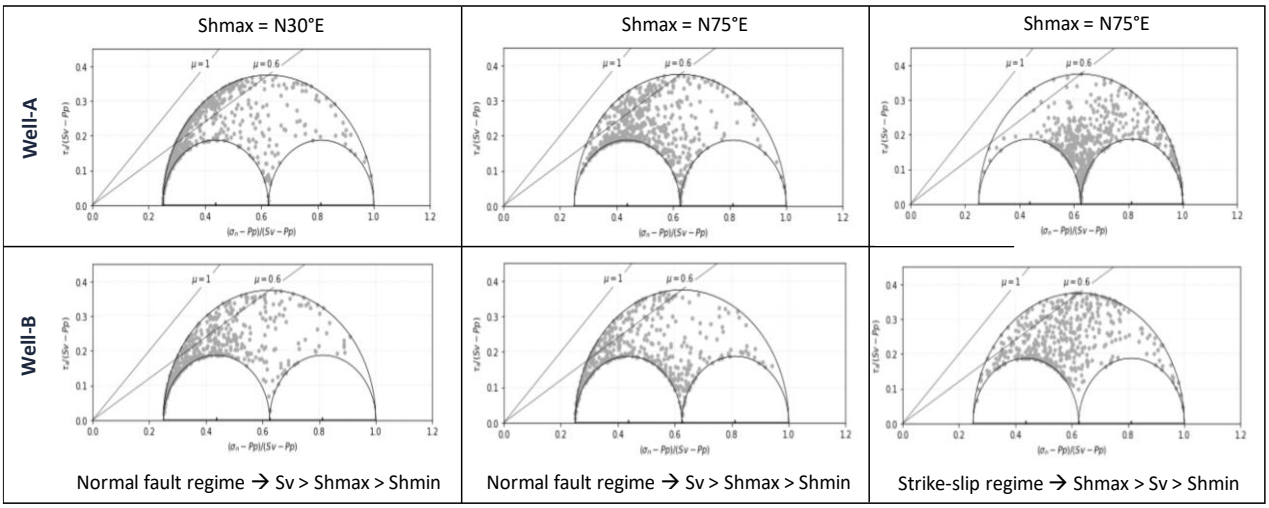

Figure 5: 3D Mohr plots of the conductive fractures in image log to identify the stress regime in the local Tompaso area.

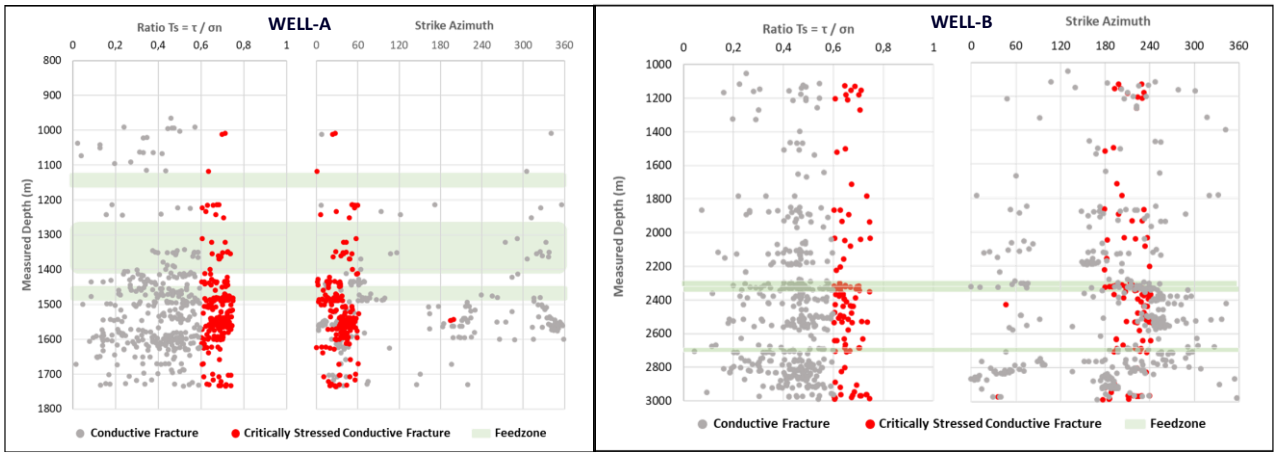

Figure 6: Critically-stressed conductive fractures in normal regime (Andersonian) with Shmax oriented to N30°E and their orientation analysis from image log data

The fracture stability analysis indicates the NE-striking fractures as the critically stressed fractures. Figure 6 shows the critically stressed conductive fractures in the normal regime model in both wells that are dominantly oriented to NE-SW, relatively parallel with the maximum horizontal stress orientation. Therefore, the geomechanics analysis in the local Tompaso area confirms the normal stress regime as the main control in the tectonic setting instead of the strike-slip regime as interpreted previously in many literatures. This NE-SW fractures also interpreted control the fluid flow in Tompaso geothermal field, both in well-scale and reservoir scale, and essential to update the Tompaso geothermal conceptual model, which still assumes the Soputan fault as the main reservoir-scale permeability control which drives the fluid from G. Sempu upflow area to the G. Umeh outflow area as discussed in Sardiyanto et al. (2015), Sidqi and Utami (2018), Lesmana et al. (2019) and Utami et al. (2020).

ISSN 2703-4275

4. TONDANO CALDERA MECHANISM

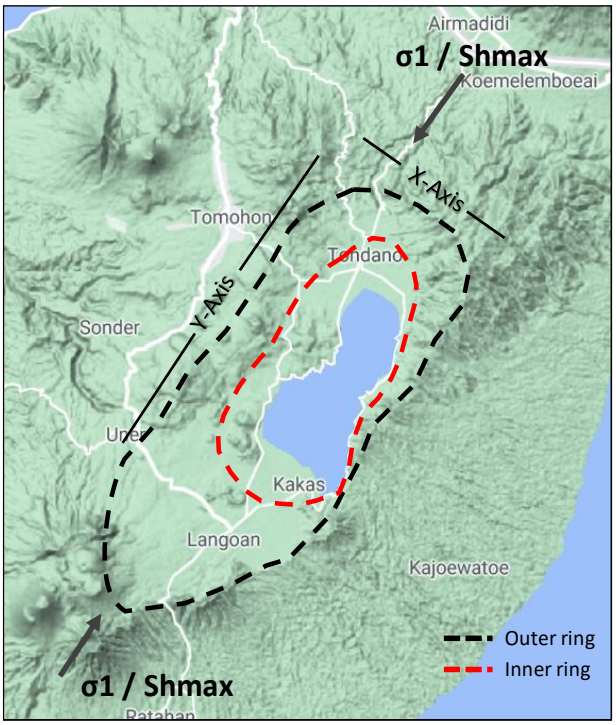

Figure 7. The ellipsoidal shape of Tondano Caldera elongate parallel with the maximum horizontal stress. Basemap credit to Google Maps.

As the Minahasa district's local data prove the subsurface structure with inferred surface structure, we propose an update of tectonic control that may relate with the forming of Tondano caldera and the local geothermal system of the Tompaso area. Acocella (2007), based on the laboratory experiment, suggests the natural caldera process mostly follows the regional tectonic trend and elongates parallel with the σ1 direction. The combination of W-E subduction of North Sulawesi subduction and the N-S subduction of East Sangihe may result in the NE-SW trends as the maximum horizontal stress in the eastern end of the North Sulawesi arm. This hypothesis may be reflected by the Tondano caldera's shape, either from the outer ring or the caldera's inner ring. Instead of expressing the polygonal shape, the Tondano caldera is more ellipsoidal, which elongates parallel with the NE-trending faults (Figure 7). The y-axis length is more than double the x-axis, where the NE-trending Lengkoan faults act as one of the western y-axes. The surface and subsurface local data have confirmed the existence of such faults that we infer as the transfer fault that accommodates the connection between Amurang – Malompar and Manado – Kema fault. As these two parallel strike-slip faults trend to NW-SE, the NE-striking faults may also represent the antithetic of the main NW-trending fault with acute angle ~70° - ~90°. These strike-slip faults sense of movement is difficult to interpret, as most of the surface fault trace is covered by the younger volcanic deposit. Nevertheless, we believe the movement tend to be left-lateral strike-slip fault based on the shape of the western coastline of Minahasa. The NE-trending may also be influenced by the double subduction of Sangihe and North Sulawesi, which is proved by the series of Quaternary volcanic occurrences follow the permeable NE-SW faults zone. The NE-trending fault zone also contributes to the hydrothermal flow in the local Tompaso geothermal system.

Assuming the Tondano caldera due to the pull-apart mechanism is difficult due to the lack of ENE-WSW faults evidence, both in surface and subsurface data. Therefore, we interpret the Tondano caldera as a classic collapse caldera where the shape follows the regional NE-trending pre-existing faults. These faults zone may also bind the caldera both in the west and eastern areas, but the surface and subsurface evidence are mostly uncertain due to the covering of the younger volcanic products, especially in the western part. The existence of the ENE-WSE fault may occur later, which intersects the northwest area of the Minahasa district extent to the Lokon – Empung volcanic complex. However, such structure may have no direct contribution to the Tondano caldera-forming process.

CONCLUSION

The tectonic setting in the Minahasa District results in an ambiguous geological framework, but identifying the existing geologic trace is doable. As our focus in the Tompaso geothermal field, we define the dominant influence of NE-striking fractures onto the fluid flow both in reservoir and well-scale. Analysis of detail surface topography data prefers to show the NE-striking faults in the vicinity of the Tompaso field. The borehole image log analysis suggests the ~ 035°- 050° conductive fractures are abundant in the wellbore, where those fractures also have been confirmed and weren't sampled as geometric sample bias. The geomechanics analysis through the drilling-induced fracture rotation also suggests that the NE-striking fractures represent the reservoir's active fracture zone. Therefore, most of the productive reservoir intervals in the Tompaso field are produced from the fracture zone with such orientation. The fracture stability analysis confirms the normal stress regime in the Tompaso area, instead of being controlled by a major strike-slip fault regime. The future well targeting in Tompaso, or even Lahendong as the neighbour field could consider this suggestion. However, the variety of local structural settings and permeability types that exists in both fields are essentially needed to be well-defined. We also suggest that the Tondano caldera-forming process followed the NE-striking faults mechanism, as the main structure that parallels the maximum horizontal stress, which represents by its ellipsoidal shape and elongation. We interpret that such fault trend results from the interaction between the double subduction in the north and eastern area of the Minahasa district.

ACKNOWLEDGEMENTS

We acknowledge PT. Pertamina Geothermal Energy provided data and permission to publish this paper. We thanks Irene Wallis for providing the Python code for the 3D Mohr plot and geomechanics modelling.

REFERENCES

Acocella, V.: Understanding caldera structure and development: An overview of analogue models compared to natural calderas. Earth-Science Reviews. https://doi.org/10.1016/j.earscirev.2007.08.004. (2007).

Barton, C. A., Zoback, M. D., and Moos, D.: Fluid flow along potentially active faults in crystalline rock: Geology, v. 23, p. 683-686. (1995).

Effendi, A.C., and Bawono, S.S.: Geologic Map of the Manado quadrangle, Noth Sulawesi, 1:250.000 scale, Geological SurveyIndonesia, Bandung, (1997).

Ezer, P.: Drilling Induced Fracture (DIF) Characterization and Stress Pattern Analysis of the Southern McMurdo Sound (SMS) Core , Vitoria Land Basin , Antarctica. Research Experience in Solid Earth Science for Students. (2008).

Hall, R., & Wilson, M. E. J.: Neogene sutures in eastern Indonesia. Journal of Asian Earth Sciences. https://doi.org/10.1016/S1367-9120(00)00040-7. (2000).

Hamilton, W. B.: Tectonics of the Indonesian region. USGS Prof. Paper 1078, 345 pp.; reprinted with corrections 1981 and 1985 (1979).

Ikhwan, M.: Geological Model and Permeability Framework of Bukit Daun Geothermal Field, Indonesia. Master Thesis of University of Auckland, New Zealand. (2020).

Lécuyer, F., Bellier, O., Gourgaud, A., & Vincent, P. M.: Active tectonics of north-east Sulawesi (Indonesia) and structural control of the Tondano caldera. Comptes Rendus de l'Academie de Sciences - Serie IIa: Sciences de La Terre et Des Planetes. https://doi.org/10.1016/S1251-8050(97)89462-1. (1997).

Lesmana, A., Pratama, H. B., Ashat, A., Saptadji, N. M., & Gunawan, F.: An Updated Conceptual Model of the Tompaso Geothermal Field Using Numerical Simulation. Proceedings 41st New Zealand Geothermal Workshop. (2019).

Katili, J. A.: Tectonic evolution of eastern Indonesia and its bearing on the occurrence of hydrocarbons. Marine and Petroleum Geology. https://doi.org/10.1016/0264-8172(91)90046-4. (1991).

Pertamina Geothermal Energy (PGE).: Fracture Study of Well Well-A based on Borehole Resistivity Imaging: Pertamina Geothermal Energy Internal Report. (2009).

Pezzati, G.: The Poso Basin in Gorontalo Bay, Sulawesi: Extension Related to Core Complex Formation on Land. https://doi.org/10.29118/ipa.0.14.g.297. (2018).

Sardiyanto, Nurseto, S. T., Prasetyo, I. M., Thamrin, M., & Yustin Kamah, M.: Permeability Control on Tompaso Geothermal Field and Its Relationship to Regional Tectonic Setting. In Proceedings World Geothermal Congress. (2015).

Satyana, A. H., Faulin, T., & Mulyati, S. N.: Tectonic Evolution of Sulawesi Area: Implications for Proven and Prospective Petroleum Plays. Proceeding JCM MAKASSAR. (2011).

Siahaan, E. E., Soemarinda, S., Fauzi, A., Silitonga, T., Azimudin, T., & Raharjo, I. B.: Tectonism and Volcanism Study in the Minahasa Compartment of the North Arm of Sulawesi Related to Lahendong Geothermal Field , Indonesia. Proceedings World Geothermal Congress. (2005).

Sidqi, M., and Utami, P.: The Geology and Geothermal Systems of the Minahasa District, North Sulawesi, Proc. The 6th Indonesia International Geothermal Convention and Exhibition (IIGCE) 2018, Jakarta, 5th – 8th August, 2018, 348 p. (2018).

Szentpéteri, K., Albert, G., & Ungvári Z.: Plate tectonic and stress-field modelling of the North Arm of Sulawesi (NAoS), Indonesia, to better understand the distribution of mineral deposit styles. (2015).

Terzaghi, R. D.: Sources of error in joint surveys. Geotechnique. https://doi.org/10.1680/geot.1965.15.3.287. (1965).

Townend, J., & Zoback, M, D.: How faulting keeps the crust strong. Geology. https://doi.org/10.1130/0091-7613(2000)28<399:hfktcs>2.0.co;2. (2000).

Utami, P., Sidqi, M., Siahaan, Y., Shalihin, M. G. J., Siahaan, E. E., & Silaban, M.: Geothermal Prospects in Lahendong Geothermal Field of the Tomohon – MinahasaVolcanic Terrain (TMVT), North Sulawesi, Indonesia. World Geothermal Congress 2020 Reykjavik, 26 May-2 April 2020, p. (2020).

Wallis, I.C., Rowland, J. V. and Dempsey, D. E., Allan, G., Sidik, R., Martikno, R., McLean, K., Sihotang, M., Azis, M. and Baroek, M.: Approaches to imaging feedzone diversity with case studies from Sumatra, Indonesia, and the Taupo Volcanic Zone, New Zealand. New Zealand Geothermal Workshop: Waitangi, New Zealand. (2020).

Wardhani, A, K, D., Sastranegara, R, M, T., Hendriansyah, T., Agung, L., Haq, F, D., Suryanto, S., & Raharjo, I, B.: Fault Characterization in Tondano Depression Using Focal Mechanism Analysis. World Geothermal Congress. (2020F).

Zoback, M. D., Prescott, W. H., & Krueger, S. W.: Evidence for lower crustal ductile strain localization in southern New York. Nature. https://doi.org/10.1038/317705a0. (1985).

Zoback, M. D.: Reservoir Geomechanics. In Reservoir Geomechanics. https://doi.org/10.1017/CBO9780511586477. (2010)